Effects of temperature and temperature gradient on concrete performance at elevated temperatures

Quang X. Le[1,2], Vinh T. N. Dao[1,a], Jose L. Torero[1], Cristian Maluk[1], Luke Bisby[3]

---

[1] *School of Civil Engineering, The University of Queensland, Brisbane, Australia.*

[2] *Faculty of Civil Engineering, The University of Danang – University of Science and Technology, Danang, Vietnam.*

[3] *School of Engineering, University of Edinburgh, Edinburgh, UK.*

[a] Corresponding author: v.dao@uq.edu.au

Abstract

To assure adequate fire performance of concrete structures, appropriate knowledge of and models for performance of concrete at elevated temperatures are crucial yet currently lacking, prompting further research. This paper first highlights the limitations *of* inconsistent thermal boundary conditions in conventional fire testing; and *of* using constitutive models developed based on empirical data obtained through testing concrete under minimised temperature gradients *in* modelling of concrete structures with significant temperature gradients. On that basis, the paper outlines key features of a new test setup using radiant panels to ensure well-defined and reproducible thermal and mechanical loadings on concrete specimens. The good repeatability, consistency and uniformity of the thermal boundary conditions are demonstrated using measurements of heat flux and in-depth temperature of test specimens. The initial collected data appear to indicate that the compressive strength and failure mode of test specimens are influenced by both temperature and temperature gradient. More research is thus required to further quantify such effect and also to effectively account for it in rational performance-based fire design and analysis of concrete structures. The new test setup reported in this paper, which enables reliable thermal/mechanical loadings and deformation capturing of concrete surface at elevated temperatures using digital image correlation, would be highly beneficial for such further research.

Keywords

concrete; elevated temperatures; heat flux; temperature gradient; strength; furnace; constitutive models.

1 Introduction

The outbreak of fire in buildings and civil engineering structures can have disastrous consequences, including severe structural damage, significant loss of contents and possible loss of life. Adequate design for fire is thus an essential requirement in the design process and can be achieved by active, non-structural measures coupled with passive, structural means. The structural design objectives are to ensure that none of the three main fire-related limit states (being strength, insulation and fire integrity) is reached in less than a specified time, called fire-resistance period.

Being the most commonly used construction material, concrete has favourable inherent characteristics with respect to fire, including: low thermal conductivity, high heat capacity, non-combustibility, and no emission of smoke or toxic gases. High levels of fire resistance for traditional concrete structures can thus commonly be achieved by adopting certain member dimensions and cover to reinforcement (Australian Standard, 2009). Nevertheless, concrete also exhibits some less attractive aspects when exposed to elevated temperatures, including degradation of material properties and spalling (Dao, 2014; Khoury, 2000). Consequently, both the load-carrying and separating/insulating functions of concrete structures could be compromised.

Despite extensive research in the past decades, our current knowledge of fundamental properties of concrete at elevated temperatures remains largely based on data from conventional tests in which the thermal loading experienced by concrete specimens remains difficult to be consistently controlled (Torero, 2014; Maluk et al., 2014; Maluk et al., 2012; Le, 2016). As a result, the effect of temperature and temperature gradients on the fire performance of concrete structures has not been adequately investigated. Accordingly, the influence of critical processes linked with temperature and its gradients, including thermal stresses, moisture transport and pore pressures, has not been properly addressed. This knowledge gap is critical considering the likely significant temperature gradients within concrete in fires (Torero, 2014; Dao, 2014).

As a result, revised knowledge of fundamental properties of concrete at elevated temperatures is required. This is especially so in the context of current strong movement towards performance-based design for fire-related applications.

The success of such movement hinges firstly on the establishment of critical solution-enabling knowledge/tools, of which reliable numerical modelling is a critical component. Reliable numerical modelling, in turns, requires realistic constitutive models that should (i) reflect the true performance of concrete material at elevated temperatures and (ii) be based on reliable and well-documented results from tests carried out under well-defined and well-controlled conditions.

This paper first clearly highlights major shortcomings of "standardized" conventional tests for concrete in fire and accordingly limitations in currently available constitutive models for concrete at elevated temperatures. On that basis, key features of a newly-developed test system using radiant panels to impose consistent thermal and mechanical loadings on concrete specimens are reported. Initial results generated using the new setup are also presented, together with their discussion and suggestions of further work.

2 Limitations of thermal boundary conditions on specimens in conventional test and their effects

The increase of temperature in a test specimen is directly related to the incident heat flux on the specimen's surface. When a conventional fire testing furnace/oven is used, the temperature evolution of the gases in the furnace is controlled (if thermocouples are used) and the heat-flux to a plate (if a plate thermometer is used). The net heat flux at the specimen's surface results from a combination of radiation and convection between the furnace environment and the test specimen. This complex heat transfer process may be further complicated by the presence of other test specimens within the testing chamber.

Through consideration of energy balance, the net heat flux at the specimen's surface q''_{net} can be approximated as (Maluk et al., 2016):

$$q''_{net} = F_{g,s}.\varepsilon_g.\sigma.T_g^4 + h_c(T_g - T_s) - \alpha_s.\sigma.T_s^4 \quad (1)$$

where, $F_{g,s}$: view factor of the compartment to specimen surface; T_g, T_s: temperature of the gas and of specimen surface; α_s: absorptivity of the gases inside furnace/oven; ε_g: emissivity of the gases; σ: the Stefan-Boltzmann constant; h_c: average convective heat transfer coefficient of both radiation and convection modes of gas.

The evolution of q''_{net} in time and space is thus highly complex, and accordingly very difficult to be controlled accurately and consistently. This inconsistent thermal loading imposed on test specimens has serious implications for the case of concrete with Biot number close to 1 (Figure 1), where proper characterisation of thermal boundary conditions is required (Torero, 2014; Bisby et al., 2013). In contrast, for the case of plasterboard with Biot number much greater than 1, T_s approximates T_g - enabling the simple adoption of the monitored gas temperature (T_g) as T_s on the specimen surface. For steel with Biot number much smaller than 1, a single temperature can be assumed for specimen, thereby significantly simplifying the problem.

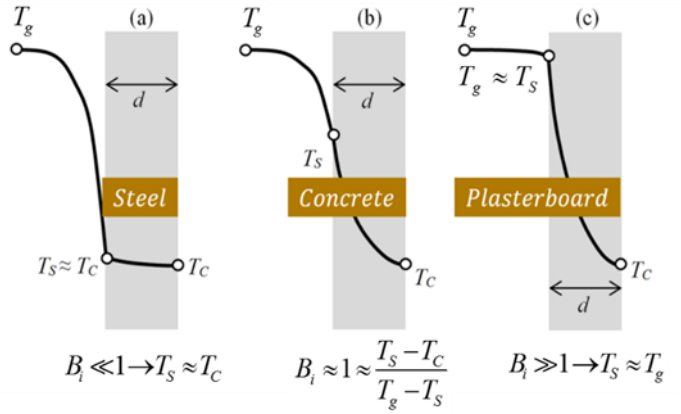

Figure 1. Typical temperature distribution for different materials.

Poor definition of q''_{net} makes it challenging to achieve reliable control of the temperature evolution as well as temperature gradient in test specimens in furnace tests. This has caused, at least partly, the following issues:

a. Significant variation in test results regarding both strength deterioration and spalling of concrete upon heating (Phan, 1996; Khoury et al., 1984): Different heating rates result in different heating histories. These are complex and generally undefined due to poor resolution of thermocouples and sensors. The undefined different heating histories in turn result in unquantifiable variability in the responses of test specimens. The significant variation in test results is likely also due in part to the inherent variation of concrete properties, and partly to possible experimental errors. In conventional tests, as a result of the limitations in thermal loading highlighted above, it is difficult to assess contributions from different sources of errors.

b. Currently available constitutive models for concrete have largely been derived from standardized tests where temperature gradients within the concrete test specimens is intentionally minimised (Phan, 1996; Cheng et al., 2004), with the aim being to separate, as far as possible, the "material" effects from the "structural" effects (Khoury et al., 1984). Limitations of these constitutive models include:
   - Mass transfer processes affected by heat are different from typical real fire situations (with higher temperature gradients) because the very slow heating rates not only allow dissipation of heat through the specimen but also slow dissipation of water vapour with minimal pore pressure increase.
   - Components of the model linked with temperature gradients have not been explicitly addressed, nor have the couplings between different processes linked to temperature gradients (including moisture transport, vapour pressure and thermal gradient induced stresses).

It is thus questionable whether such constitutive models developed based on tests under minimised temperature gradients are representative of concrete in structures with substantial temperature gradients.

A research program is thus underway at The University of Queensland to re-examine the thermal and mechanical performance of concrete at elevated temperatures by establishing well-defined and consistently-controlled thermal boundary conditions. This paper reports initial results of material testing of cylinder specimens, forming the basis for revision of constitutive models to better reflect the effects of temperature and temperature gradients.

3 Experimental study

3.1 Test specimens and materials

Concrete cylinders of Φ100mmx200mm were adopted due to their common use for establishing uniaxial constitutive models of concrete in compression. The mix design was typical for concrete with 28-day compressive strength of 80 MPa, and is given in Table 1. All mixing and casting was done in accordance with relevant Australian standards (AS 1012.1:2014, 2014). A photo of moulds assembled on the vibrating table ready for casting is shown in Figure 3.

To ensure consistent moisture conditions, upon stripping from their moulds one day after casting, test specimens were cured in water at 27^{o}C for four months, and then in the controlled room of 27°C and 70% relative humidity (Figure 4) for another three months until testing. The mass loss with time was monitored and found to become negligible after about 40 days, indicating that the test specimens had reached moisture equilibrium with the ambient air in the controlled room.

Table 1. Concrete mix design.

Constituents	Quantity (/m^3)
10mm aggregate	925 (kg)
Manufactured coarse sand	600 (kg)
River fine sand	140 (kg)
Cement	580 (kg)
Water	193 (l)
Superplasticiser	4.06 (l)

Two series of specimens were prepared, including:

- Series 1, of 9 specimens with internal thermocouples: Each specimen had 5 thermocouples located on two radial lines at mid-height. Temperatures were measured at three depths (Figure 2): (i) at the specimen's surface and (ii) centreline, and (iii) at 21 mm from the surface; this being the location of the average temperature (Le et al., 2015). The thermocouples used in this experiment were Type K with good moisture, chemical and abrasion resistance. The thermocouples were 20-gauge (0.965 mm diameter), grade, and solid wire. The thermocouples also contained high-temperature fibreglass braid single conductors and duplex insulation. The maximum temperature of a single thermocouple is 705°C for continuous temperatures, and 870°C for a single reading. The specific limit of error is ±0.75% standard tolerances with temperatures from 0°C to 1260°C (Pyrosales, 2014). To locate the thermocouples at intended positions, a welding wire frame (Figure 2) was used.
- Series 2, of 33 specimens without thermocouples: Specimens were exposed to pre-determined schemes of heat flux boundary condition before testing to failure under compression. Due to good repeatability of heating and curing, temperature profiles in these specimens were assumed the same as corresponding specimens in Series 1.

Thus, Series 1 specimens with thermocouples were to provide temperature data from which required heating time to target temperature profile under a given heat flux level could be determined. Series 2 specimens without thermocouples were to determine the load-deformation to assess the possible effects of different incident heat fluxes and thus of associated temperature and temperature gradients.

- Three additional specimens without thermocouples were also cast and cured in water at 27^{o}C until the age of 28 days for determination of the 28-day compressive strength of test concrete.

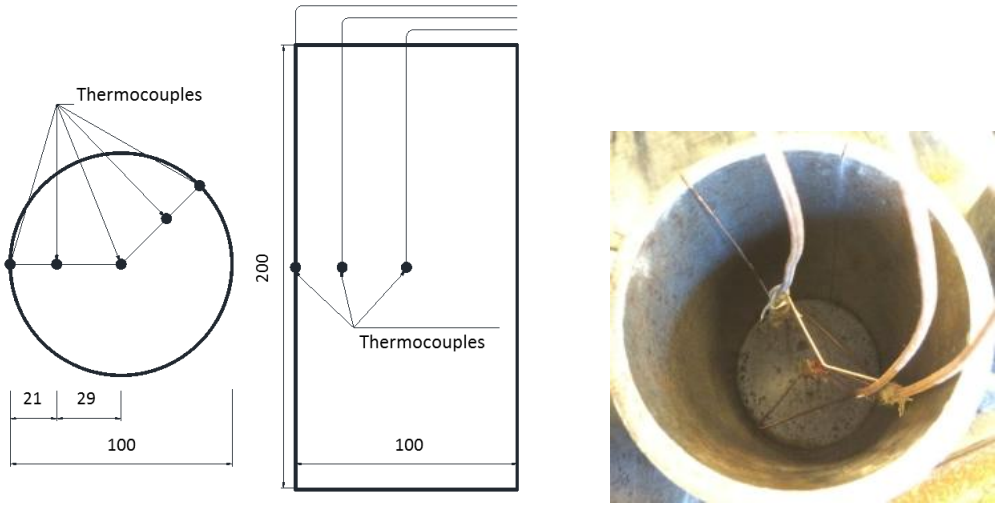

Figure 2. Locations of thermocouples in the cylinder concrete specimens.

Figure 3. Photo of moulds for both series ready for casting on the vibrating table.

Figure 4. Test specimens in the controlled room of 27°C and 70% relative humidity.

3.2 Radiant panel heating setup

The heat flux incident on cylinder test specimens was actively controlled using a system of four high performance radiant heating elements (Figure 7). Calibration of heat flux was performed using a Schmidt-Boelter heat-flux sensor as follows:

- The incident heat flux from each of the four panels was determined as a function of the distance between the panel and the target at the start of the testing, and this was repeated upon completion of the test series (Figure 5). The heat flux profiles produced by the four panels were essentially identical (Figure 6), proving that the consistency between the four panels was maintained throughout the testing.
- Two radiant panels were used to determine the degree of uniformity of incident heat flux intensities on the cylinder specimen surface placed at different offset distances (Figure 5). The measured heat fluxes at the three locations (i.e. A, B and C) varied within by 5% for all distances, prompting a homogeneous thermal boundary condition around the curve surface of cylinder test specimen.

3.3 Imposed heat fluxes and target temperatures

Following the above calibration process, the incident heat flux intensities in this study were chosen within the typical range for building fires (Federation Internationale du Beton, 2007) as 20, 30, and 40 kW/m^2 (denoted subsequently in

this paper as HF20, HF30 and HF40). Concrete specimens were first heated under a given incident heat flux level until the target average temperature, as recorded by thermocouples at 21 mm depth from the specimen surface, was reached (Figure 7). Besides ambient temperature, four target temperatures (150^{o}C, 300^{o}C, 450^{o}C and 600^{o}C) were chosen to capture the effects of major physico-chemical changes in concrete specimens at elevated temperatures (Khoury, 2000; Hertz, 2005; Baker, 1996; Dao, 2014). Once a given target temperature was reached, the test specimens were loaded in compression at a rate of 0.25 mm/min until failure.

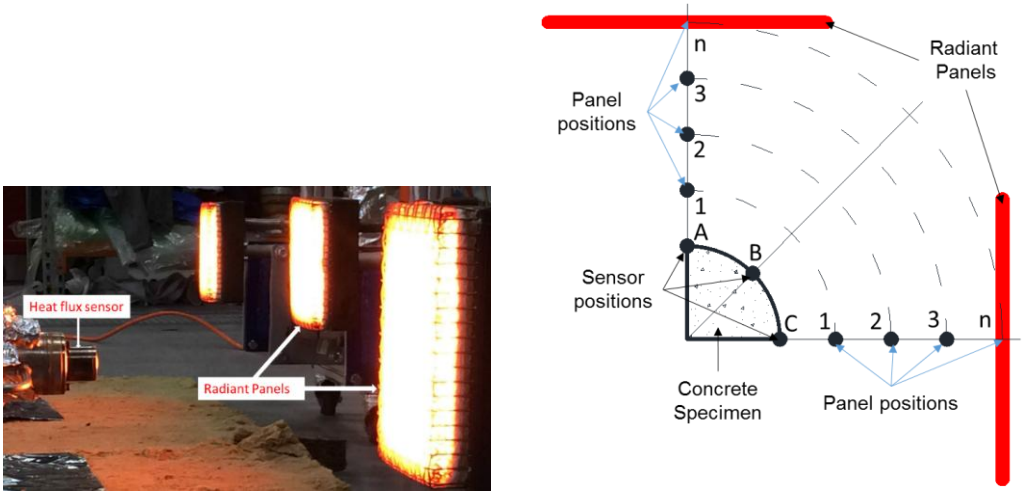

Figure 5. Illustration of heat flux calibration process.

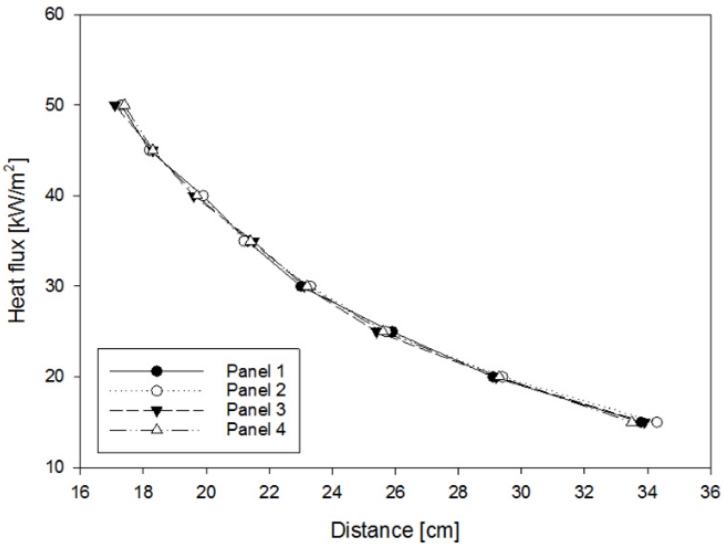

Figure 6. Variation of heat flux with distance from the radiant panel surface.

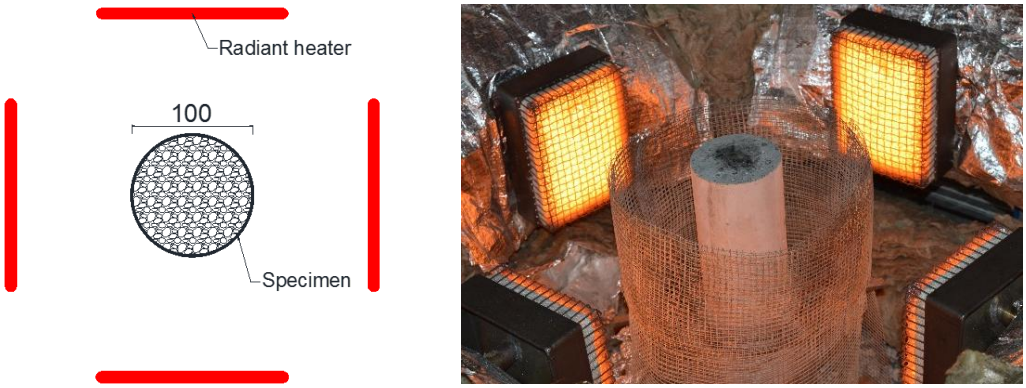

Figure 7. Arrangement of four radiant heaters around cylinder test specimen.

3.4 Mechanical loading preparation

Figure 8 shows a schematic of the test setup for mechanical and thermal loading. Key features of the test setup include:

- Loading crossheads below and above the test specimen: A water-cooling system was designed to maintain the temperature of the crossheads at less than 40°C during testing. The concrete blocks, as part of the top and bottom water-cooled attachments, were made of 100 MPa concrete and had dimensions of ϕ127mmx95mm, acting as an insulator with similar thermal conductivity to that of test specimens.
- A spherical seat ensured that uniaxial compression load was imposed.
- A steel mesh of 5mm x 5mm grid was placed around the test specimens to protect the radiant panels from possible explosive spalling (Figure 7).
- Since the radiant panels required around 5 minutes to reach their stable thermal state, the test specimens were initially covered in a hollow cylinder of 110mm in inner diameter and 210mm in height. This hollow cylinder was made of Rockwool with very low thermal conductivity and further wrapped in aluminium foil with high reflectivity to ensure no heating of test specimens during the initial warming-up period of the radiant panels.

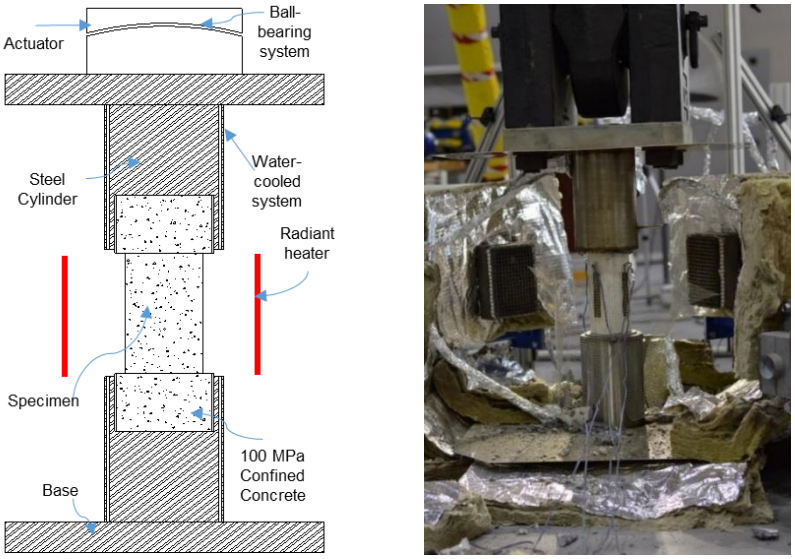

Figure 8. Schematic illustration and photo of test setup.

4 Results and discussion

4.1 Spalling

No spalling was observed during testing of all 39 concrete specimens in both Series 1 and Series 2 at elevated temperatures. Such no spalling was interesting considering the high concrete compressive strength of test specimens nearly 100 MPa on test date and the significant rate of temperature increase within specimens of up to 30 °C/min in this study. Further work is therefore needed to shed more light onto underlying mechanisms for concrete spalling in fire. The highly consistent, reliable and repeatable thermal boundary conditions through using the radiant panel heating setup as demonstrated in this research (§3.2) would be beneficial in such study.

4.2 Time evolution of in-depth temperature profiles

The time evolution of in-depth concrete temperature profiles in three test specimens was determined for each of the three incident heat flux levels. A good degree of consistency was observed among the measured temperatures for each heat flux (Figure 9). The recorded temperatures along the two radial lines at corresponding depths also had good agreement, further confirming the uniform heat flux boundary condition.

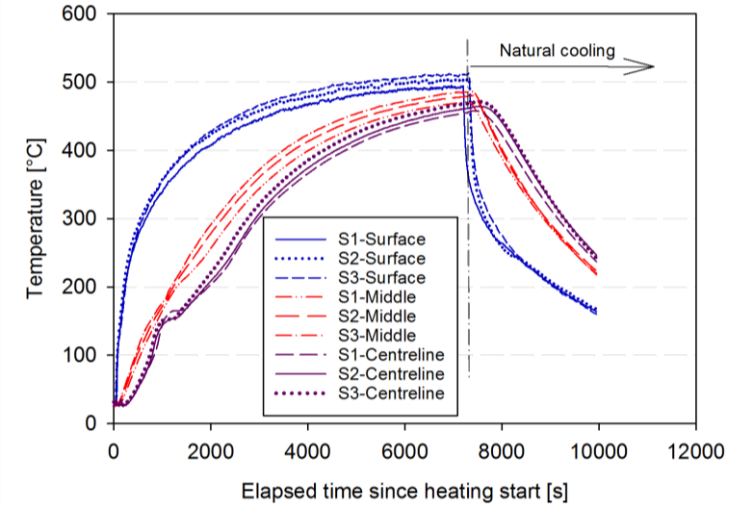

a. For heat flux of 20 kW/m^2.

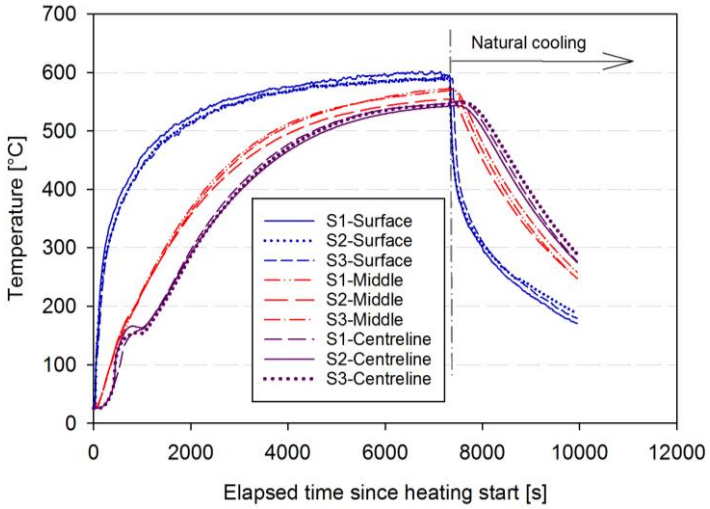

b. For heat flux of 30 kW/m^2.

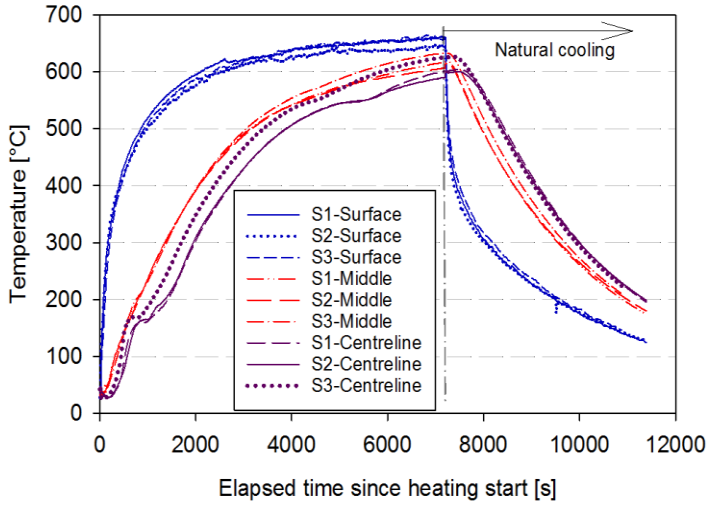

c. For heat flux of 40 kW/m^2.

Figure 9. Temperature development at three depths of the three specimens heated by heat fluxes of 20, 30 and 40 kW/m^2.

4.2 Colour change, water evaporation and failure mode of test specimens

When subjected to high temperature, concrete specimens would experience colour change, cracking and possible spalling (Arioz, 2007). Figure 10 shows a typical change of colour due to the temperature increase in different layers concrete specimens in this study – when a concrete specimen heated by essentially uniform heat flux boundary conditions. The surface concrete of about 10 mm thick appeared much darker than concrete in the inner layer. In addition, network of fine cracks was observed on the surface of test specimens, especially for the case of incident heat flux of 40 kW/m^2.

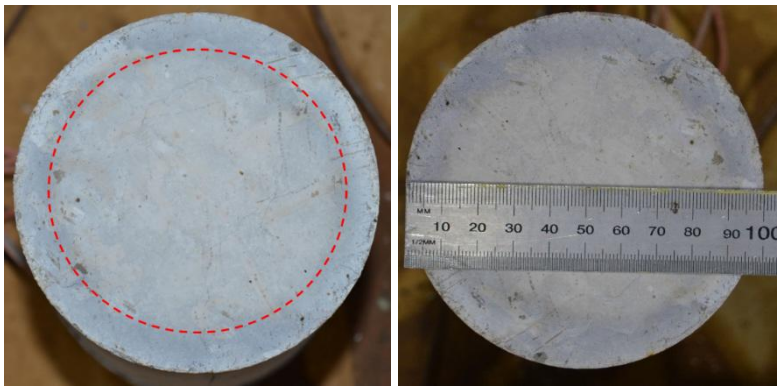

Figure 10. Different colour change due to surface heating.

Shortly after test specimen's exposure to a given incident heat flux, water was observed coming out of the top and bottom surfaces of the specimen, as shown in Figure 11. Significant moisture accumulation was clearly observed on specimen's top surface from around 15, 10 and 5 minutes after heating for incident heat flux of 20, 30 and 40 kW/m^2, respectively. The specimen's top surface was also seen to be completely dried after being heated for about 31, 22 and 17 minutes.

Figure 11. Water migration/bleeding on top of the specimen surface.

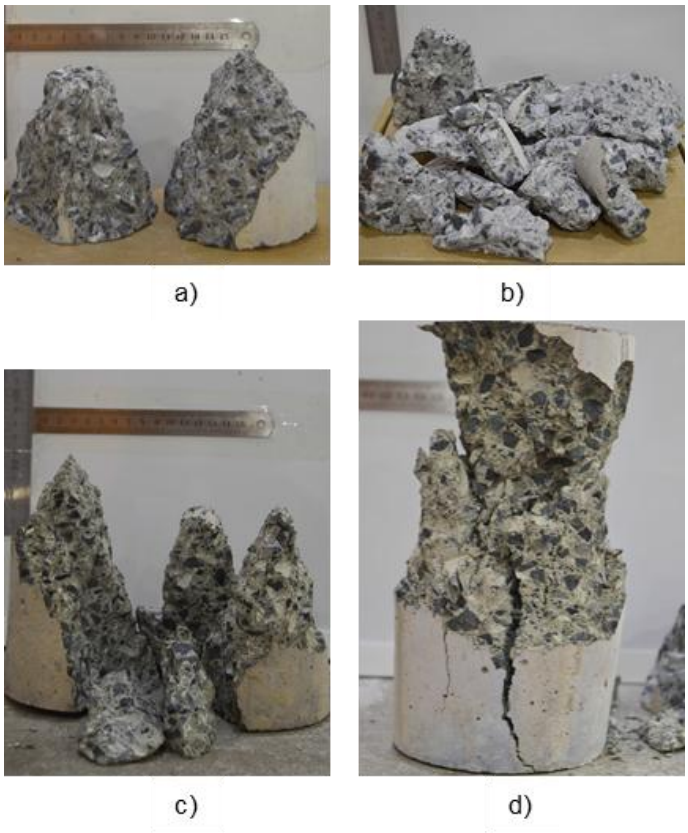

Figure 12. Failure mode of specimens at: a. 150°C; b. 300°C; c. 450°C; d. 600°C.

The typical failure modes of cylindrical concrete specimens at different target temperatures are given in Figure 12:

- At target temperatures of 150°C and 450°C, reasonable well-formed cones at the two ends of cylindrical specimens were observed at failure;
- However, at 300°C, specimens were completely broken into small pieces;
- At 600°C, a well-formed cone was observed only at one end, together with vertical cracks running through the other end.

Interestingly, the failure mode of all test specimens at a particular target temperature was observed to be consistently similar. It is hypothesised that such failure modes were influenced by thermal stresses associated with different heat fluxes and temperature gradients – Further research is needed to ascertain the underlying reasons for these observed failure modes.

4.3 Strength of concrete at elevated temperatures

The compressive strength at ambient temperature at 28 days and on test dates were 82.4 MPa and 97.4 MPa, respectively. For elevated temperatures, three cylinder specimens were tested for each combination of incident heat flux and

target temperature. The average compressive strengths at different target temperatures and incident heat fluxes, normalized against corresponding test-date strengths at ambient temperature, are plotted in Figure 13.

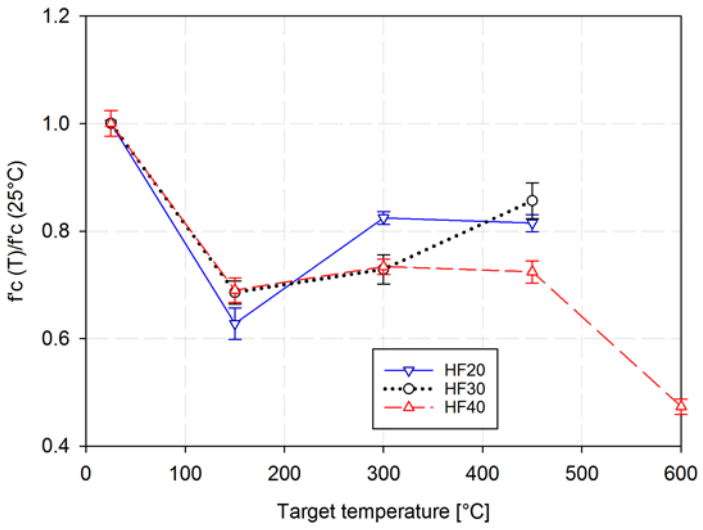

Figure 13. Change of concrete compressive strength at different target temperatures and incident heat fluxes.

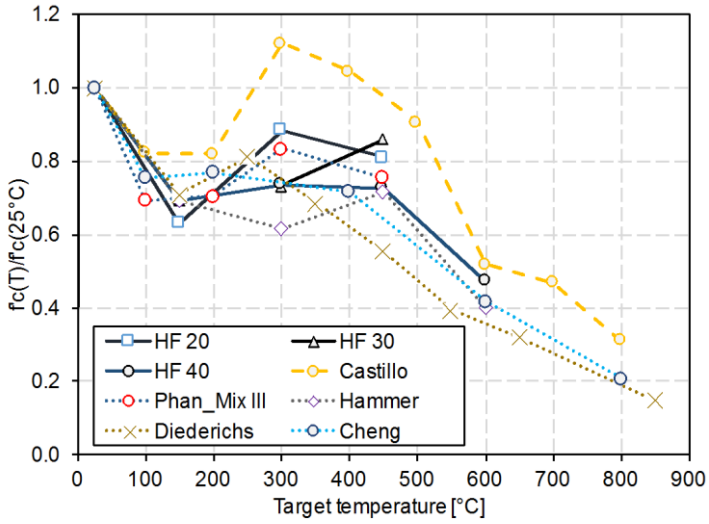

Figure 14. Comparison of compressive strengths in current and comparable previous studies.

It is evident from Figure 13 that at a given target temperature and heat flux, the variation of concrete strength was small. Compared to relevant results from comparable previous studies (Figure 14) (Hammer, 1995; Phan and Carino, 2001; Castillo and Durrani, 1990; Diederichs et al., 1988; Cheng et al., 2004), compressive strengths obtained in this work appear to follow similar trend, but

with considerable smaller variation. Besides the highly consistent casting and curing conditions for all specimens, such small variation was likely due to the consistent thermal loading, which was made possible by the newly-developed test setup in this study.

Importantly, it can also be seen from Figure 13 that, at a given average elevated temperature, concrete strengths of test specimens subject to different incident heat fluxes differ significantly. Such a difference can be explained by linking temperature gradients, heating time, and corresponding physico-chemical processes within concrete specimens. At an average temperature of 300°C, for instance, the temperature ranges within test specimens due to heat fluxes of 20, 30 and 40 kW/m^2 were 233 to 431, 217 to 490, and 212 to 545°C, respectively. As a result, while significant strength recovery was observed in HF20 specimens due to increased surface forces arising from loss of absorbed water (Cheng et al., 2004), such recovery was modest in HF30 and HF40 specimens, possibly due mainly to the counteracting effect of decomposition of $Ca(OH)_2$ (Khoury, 1992; Arioz, 2007).

Figure 13 accordingly indicates the potential influence of incident heat fluxes, and thus the associated temperature and temperature gradients, on concrete properties at elevated temperatures. The challenging question is to quantify such influence and also to develop methodology to effectively account for it in fire design and analysis of concrete structures. The test setup as reported in this paper, which allows to apply reliable thermal and mechanical loadings on specimens, would be highly beneficial for such further research.

Importantly, the new setup also enables reliable non-contact full-field deformation capturing of concrete surface at elevated temperatures using digital image correlation – Such deformation capturing is typically not possible in conventional test setups (Le et al., 2017). The combined advantages of the above would allow to generate required reliable data, thereby enabling the development of effective rational fire design and analysis of concrete structures.

5. Summary and conclusions

This paper has highlighted the limitations of: (i) inconsistent thermal boundary conditions in conventional fire testing; and (ii) the adoption of constitutive models

developed based on tests under minimised temperature gradients in modelling of structures with significant temperature gradients.

On that basis, details of a research program aiming to re-examine the fire performance of concrete structures, taking due account of temperature and temperature gradients, have been presented. The test setup for thermal and mechanical loading, using radiant panels to generate well-defined and reproducible heating regimes, has been described. The good repeatability, consistency and uniformity of the thermal boundary conditions on test cylinder specimens has also been demonstrated.

Using this test setup, initial results on fundamental mechanical properties including compressive strengths of concrete specimens at various target temperatures under different heat flux intensities have been measured and reported. At a given target temperature, the measured compressive strengths and failure modes of test specimens have been observed to be influenced by the time-history of thermal boundary conditions, implying an observable effect of temperature gradients on concrete properties at identical average elevated temperatures. Further research is ongoing to quantify this effect and also to develop methodologies to effectively account for it in rational performance-based fire design and analysis of concrete structures.

Acknowledgements

The authors acknowledge the financial support of Australian Research Council's Discovery Projects funding scheme (DP150102354). The first author is also grateful for the financial support of Australia Awards Scholarships.

References

Arioz O. (2007) Effects of elevated temperatures on properties of concrete. *Fire Safety Journal* 42: 516-522.

AS 1012.1:2014. (2014) Australian Standard. *Methods of testing concrete. Method 1: Sampling of concrete.* Sydney, NSW 2001: Standards Australia Limited.

Australian Standard. (2009) AS 3600-2009. Concrete structures. Standards Australia Limited: SAI Global Limited.

Baker G. (1996) The effect of exposure to elevated temperatures on the fracture energy of plain concrete. *Materials and Structures* 29: 383-388.

Bisby L, Gales J and Maluk C. (2013) A contemporary review of large-scale non-standard structural fire testing. *Fire Science Reviews* 2:1.

Castillo C and Durrani AJ. (1990) Effect of transient high temperature on high-strength concrete. *Materials Journal* 87: 47-53.

Cheng F-P, Kodur VKR and Wang T-C. (2004) Stress-strain curves for high strength concrete at elevated temperatures. *Journal of Materials in Civil Engineering* 16: 84-90.

Dao VTN. (2014) Performance of concrete in fire. *Concrete in Australia - Special Issue on "Concrete Performance in Fire"* 40(3): 50-53.

Diederichs U, Jumppanen UM and Penttala V. (1988) Material properties of high strength concrete at elevated temperatures. *IABSE 13 Congress.* Helsinki.

Federation Internationale du Beton. (2007) Bulletin 38: Fire design of concrete structures - materials, structures and modelling. 105.

Hammer TA. (1995) High strength concrete phase 3, compressive strength and E-modulus at elevated temperatures. *SP6 Fire resistance.* Trondheim.

Hertz KD. (2005) Concrete strength for fire safety design. *Magazine of Concrete Research* 57: 445-453.

Khoury GA. (1992) Compressive strength of concrete at high-temperatures - a reassessment. *Magazine of Concrete Research* 44: 291-309.

Khoury GA. (2000) Effect of fire on concrete and concrete structures. *Progress In Structural Engineering And Materials* 2: 429-447.

Khoury GA, Sullivan PJE and Grainger BN. (1984) Radial temperature distributions within solid concrete cylinders under transient thermal states. *Magazine of Concrete Research* 36: 146-156.

Le B-D, Tran S, Dao V, et al. (2017) Deformation capturing of concrete structures at elevated temperatures. *Accepted for PROTECT2017 - The Sixth International Workshop on Performance, Protection & Strengthening of Structures under Extreme Loading.* South China University of Technology, Guangdong, China.

Le QX. (2016) A study of temperature gradient effects on mechanical properties of concrete at elevated temperatures. *School of Civil Engineering.* Brisbane, Australia: The University of Queensland, 130.

Le QX, Dao VTN and Torero JL. (2015) Fire performance of concrete: Effect of temperature gradients? In: Kodur VKR and Banthia N (eds) *PROTECT2015 - The Fifth International Workshop on Performance, Protection & Strengthening of Structures under Extreme Loading.* Michigan State University, 189-196.

Maluk C, Bisby L, Krajcovic M, et al. (2016) A Heat-Transfer Rate Inducing System (H-TRIS) Test Method. *Fire Safety Journal*.

Maluk C, Bisby L and Terrasi G. (2014) Experimental parametric study on the effectiveness of polypropylene fibres at mitigating heat-induced concrete spalling. *Concrete In Australia* 40(3): 32-37.

Maluk C, Bisby LA, Terrasi G, et al. (2012) Novel fire testing methodology: Why, how and what now? *Proceedings of the Mini Symposium on Performance-based Fire Safety Engineering of Structures as part of the 1st International Conference on Performance Based land Life Cycle Structural Engineering.* Hong Kong: Hong Kong Polytechnic University, 448-458.

Phan LT. (1996) Fire performance of high-strength concrete: A report of the state-of-the-art. The National Institute of Standards and Technology (NIST), 118.

Phan LT and Carino NJ. (2001) Mechanical properties of high-strength concrete at elevated temperatures. Building and Fire Research Laboratory - National Institute of Standards and Technology.

Pyrosales. (2014) Thermocouple wire and cable. In: Pyrosales Total Sensors Solution (ed). Australia.

Torero J. (2014) Assessing the performance of concrete structures in fires. *Concrete in Australia - Special Issue on "Concrete Performance in Fire"* 40(3): 44-49.